System Modeling and Robust Control of an AMB Spindle: Part II A Robust Controller Design and its Implementation

Hyeong-Joon Ahn
Department of Mechanical & Aerospace Engineering, University of Virginia, 122 Engineer's way, Charlottesville, Virginia 22904-4746, USA
Dong-Chul Han*
School of Mechanical & Aerospace Engineering, Seoul National University, 151-745, Korea

This paper discusses an entire procedure for a robust controller design and its implementation of an AMB (active magnetic bearing) spindle, which is part II of the papers presenting details of system modeling and robust control of an AMB spindle. Since there are various uncertainties in an AMB system and reliability is the most important factor for applications, robust control naturally gains attentions in this field. However, tight evaluations of various uncertainties based on experimental data and appropriate performance weightings for an AMB spindle are still ongoing research topics. In addition, there are few publications on experimental justification of a designed robust controller. In this paper, uncertainties for the AMB spindle are classified and described based on the measurement and identification results of part I, and an appropriate performance weighting scheme for the AMB spindle is developed. Then, a robust control is designed through the mixed μ synthesis based on the validated accurate nominal model of part I, and the robust controller is reduced considering its closed loop performance. The reduced robust controller is implemented and confirmed with measurements of closed-loop responses. The AMB spindle is operated up to 57,600 rpm and performance of the designed controller is compared with a benchmark PID controller through experiments. Experiments show that the robust controller offers higher stiffness and more efficient control of rigid modes than the benchmark PID controller.

Key Words: Robust Control, Uncertainty Description and Active Magnetic Bearing

Nomenclature

A	: System matrix
$C(s)$	: Controller
d	: Plant input disturbance
D	: D scaling for the μ synthesis
e	: Error
F_l	: LFT
G, $G(s)$	: Plant
M	: General plant
n	: Noise
S	: Sensitivity function
T	: Complementary sensitivity function
u	: Controller input
w	: Controller input disturbance
W	: Weighting functions
δ	: Parameter variation
ω	: Natural frequency
ξ	: Damping

* Corresponding Author,
E-mail: dchan@amed.snu.ac.kr
TEL: +82-2-880-7139; **FAX**: +82-2-883-1513
School of Mechanical & Aerospace Engineering, Seoul National University, 151-745, Korea. (Manuscript **Received** July 4, 2002; **Revised** July 1, 2003)

1. Introduction

Active magnetic bearing (AMB) systems have been widely applied due to their unique advantages such as: non-contact, lubricant-free operation, possibility of high rotational speed, and controllability of the bearing characteristics. An

AMB rotor system always requires feedback control of the magnetic force for stable levitation of the rotor. Therefore, controller design plays a central role in achieving high performance of the system.

The part I presented a modeling and validation process of an AMB spindle and this part II discusses an entire procedure for a robust controller design and its implementation of the AMB spindle based on the results of the part I.

Since there are various uncertainties in an AMB system and reliability is the most important consideration for applications, robust control naturally gains attentions in this field. For example, the electromagnetic actuator behavior is intrinsically nonlinear and an approximate linear model near an operating point is used in design of a controller. As the result of the approximate nature of the model, the model is very sensitive to parameter variations and it is essential to consider such parameter variations in design a high performance controller (Kim and Lee, 1998 ; Jeon et al., 2003).

In last decade, MIMO control system design procedures have begun to be implemented on AMB rotor systems. Cui and Nonami (1992) and Nonami et al.(1994) applied H_∞ control with the mixed sensitivity performance weighting to an AMB flexible rotor system. Also, Nonami and Takayuki (1994) implemented a simple μ control to a flexible AMB rotor, which based on a rigid rotor model and additive uncertainty model. Carrere et al.(1994) used a rotor model of six flexible modes to demonstrate H_∞ control procedure theoretically. Stephens (1995) and Fittro (1998) applied the μ synthesis to an AMB milling spindle, which contained detail modeling of the system and uncertainty descriptions, and performance weighting schemes. Although their weighting schemes were theoretically justified, the resulting controller was unstable and had to be switched after initial levitation using a simple controller such as a PID control. Losch et al. (1998) applied the μ control to a 3 MW AMB boiler feed pump. They described a model reduction, a systematic way of uncertainty description, and performance weighting. Schonhoff et al. (2000) implemented the μ control to an energy storage flywheel, which included substructure modeling, an extended weighting scheme, and implementations. However, tight evaluations of various uncertainties based on experimental data and appropriate performance weightings for an AMB spindle are still ongoing research topics. In addition, there are few publications on experimental justification of a designed robust controller.

This paper discusses an entire procedure for a robust controller design and its implementation of an AMB spindle. Various uncertainties for the AMB spindle are classified and evaluated based on the experimental results of part I, and an appropriate performance weighting scheme for the AMB spindle are developed. A robust control is designed through the mixed μ synthesis based on the accurate nominal model of part I, and reduction of the robust controller is performed considering the closed-loop performances. The reduced robust controller is implemented and validated through measuring closed-loop frequency responses. The AMB spindle is operated up to 57,600 rpm and performance of the designed controller is compared with a benchmark PID controller through experiments. Experiments show that the robust controller offers higher stiffness and more efficient control of rigid modes than the benchmark PID controller.

2. Uncertainty Description

2.1 Linear state-space variation

2.1.1 Uncertainty of rigid modes due to that of open-loop stiffness

The dependence of magnetic force on the control variables is intrinsically nonlinear so an approximate linearized model, valid near an operating point, is used in design of the associated controller. Although the force-current relationship is linear near an operating point, the force displacement relationship doesn't show good linearity and the open-loop stiffness is very sensitive to small variation of the operating point. Problem is that the open-loop stiffness is the key parameter that governs unstable poles of an AMB system.

Errors related to the open-loop stiffness can be classified as nonlinearity, hysteresis and operating point error. The nonlinearity within $\pm 100\ \mu m$ is shown in Fig. 1. The relative uncertainty due to the nonlinearity is very large, which is about 9.7 %. The hysteresis is relative difference between loading and unloading of forces. The operating point error can be evaluated from the maximum deviation of measured data at four different angular locations of the rotor. The operating point error mostly comes from run-out of the rotor. The latter two errors can be seen figures in sec. 3.3 of the part I. Table 1 shows the evaluated relative errors of the open-loop stiffness based on the experiment data.

The open-loop stiffness mostly affects the real poles related to unstable rigid modes of an AMB spindle. Therefore, it is convenient to convert uncertainty of the open-loop stiffness into that of the real poles of the rigid modes for consistency with uncertainty description of the flexible modes. The variation of the real poles corresponding to the total 22% variation of the open-loop stiffness is about 10% assuming that the open-loop stiffness of two bearings is not considerably varied in asymmetry.

Table 1 Various errors of open-loop stiffness

Types of error	Values (%)
Linearization error	9.7%
Hysteresis error	0.2-2%
Operating point error	7-9%

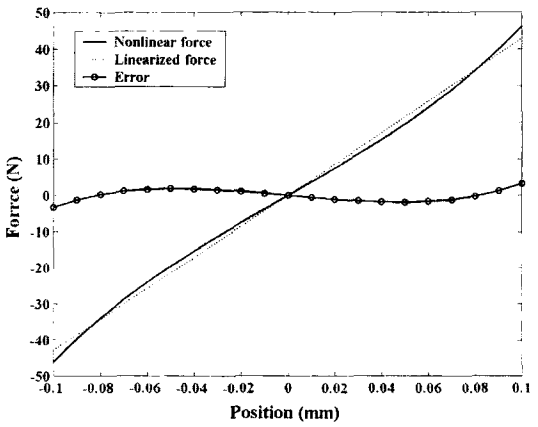

Fig. 1 The linearity error of open-loop stiffness

2.1.2 Uncertainty of bending natural frequencies

Figure 2 shows maximum additive errors of the ten times measured frequency responses of the open-loop plant in the part I. Large errors in low frequency is due to uncertainty of the rigid modes, which are already considered in the last section. In addition, there are large additive errors at the bending natural frequencies. This comes from small discrepancy in measured bending natural frequencies. Therefore, they should be modeled as parametric uncertainties of the bending natural frequencies. Here uncertainty of $\pm 3\%$ in bending natural frequencies is introduced.

2.1.3 Formulation of natural frequency uncertainties (Balas and Young, 1995)

System matrix A of a flexible mode can be transformed to a real modal representation A_i^m as follows.

$$A_i^m = \begin{bmatrix} 0 & 1 \\ -(\omega_i(1+\delta_i))^2 & -2\xi_i\omega_i(1+\delta_i) \end{bmatrix} \quad (1)$$

This is the 2×2 block of i^{th} mode and ω_i is the natural frequency with relative uncertainty δ_i. The modal damping ξ_i is considered to be constant, since it has little influence on the controller design. To linearize the nonlinear term, $(\omega_i(1+\delta_i))^2$ is approximated as $\omega_i^2+2\omega_i\delta_i$, which is

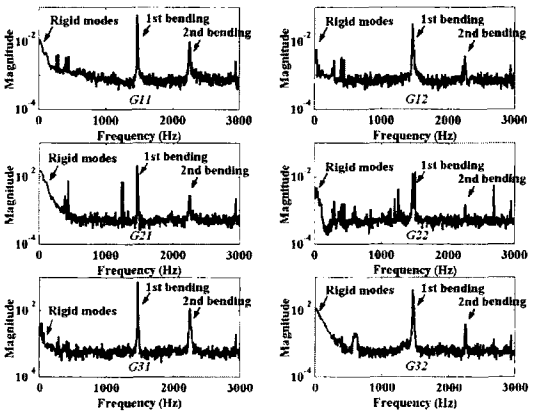

Fig. 2 Maximum additive error of ten times measured frequency responses

valid for small uncertainties. Then the system matrix can be rewritten as

$$A_i^m=\begin{bmatrix} 0 & 1 \\ -\omega_i^2-2\omega_i^2\delta_i & -2\xi_i\omega_i-2\xi_i\omega_i\delta_i \end{bmatrix} \quad (2)$$

and this uncertainty can be described in forms of the linear fractional transformation (LFT) with output and input vectors.

$$A_i^m=\begin{bmatrix} 0 & 1 \\ -\omega_i^2 & -2\xi_i\omega_i \end{bmatrix}+\begin{bmatrix} 0 \\ 1 \end{bmatrix}\delta_i\begin{bmatrix} -2\omega_i^2 & -2\xi_i\omega_i \end{bmatrix} \quad (3)$$

The uncertainty of rigid modes can be expressed in the same way as Eq. (3) if the damping ratio is neglected and the sign is inverted.

The AMB spindle is built with as small diameters as possible to increase the maximum rotational speed. This means that the gyroscopic effect is small even if the AMB rotor operates at a very high rotating speed.

2.2 Parameter variations

2.2.1 Sensor gain

Uncertainties of a sensor gain can be the linearity error, thermal drift and so on. In case of a cylindrical capacitive sensor (CCS), the linearity error is dominant since the nonlinear relationship between the displacement of a spindle and capacities is approximated using a differential configuration of the CCS (Ahn et al., 2000; Jeon et al., 2001). The 100 μm radius range in polar coordinate can be approximated by ± 70 μm range

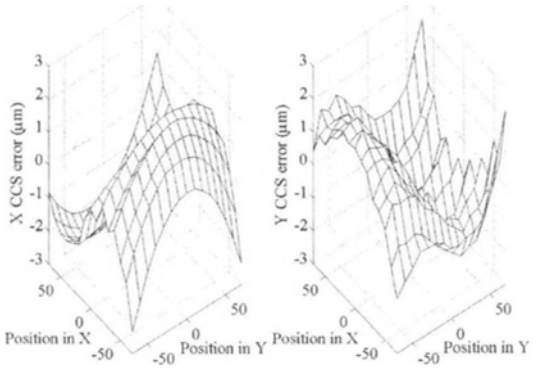

Fig. 3 Linearity errors of the front 8-segment CCS

Table 2 Various errors of current gain

Types of error	Values (%)
Linearization error	0.5%
Hysteresis error	4-6%
Operating point error	0.5-2.5%

in Cartesian coordinate. The additive linearity errors within ± 70 μm are shown in Fig. 3. The relative errors are less than $\pm 2.5\%$. The $\pm 3\%$ uncertainty of sensor gain is introduced including the thermal drift.

2.2.2 Current gain (Namerikawa, 1998)

Current gain of an AMB system contributes to static gain of the plant like the sensor gain. Through the same procedure as the open-loop stiffness, uncertainties of the current gain are evaluated as shown in Table 2. While the linearity error and operating point error is small, the hysteresis error is dominant.

2.3 Unmodeled dynamics and modeling error

Models of uncertainties are not limited to the parametric uncertainties. Often, a low-order nominal model that suitably describes the low-mid frequency range behavior of the plant is available, while high-frequency plant behavior is very uncertain. Moreover, the dynamics after 3 kHz is discarded from the nominal rotor model. Therefore, something richer than the parametric uncertainties is needed to represent this uncertainty.

Relative deviations of the ten times measured frequency responses of the part I are shown in Fig. 4. The relative deviations are linearly proportional to the frequency. Although errors near the bending natural frequencies are large, they are already considered as the parameter variations in the last section. This measured relative error can be considered as a kind of modeling error because the relative error comes form the uncertainties of model in high frequency.

One common approach for this unstructured uncertainty is to use a multiplicative uncertainty model. Roughly, this allows us to specify a frequency-dependent multiplicative uncertainty in an actual plant behavior. The precise definition of

the multiplicative uncertainty set is

$$M(G_n, W_u) \cong \left\{ G_a : \left| \frac{G_a(j\omega) - G_n(j\omega)}{G_n(j\omega)} \right| \leq |W_u(j\omega)| \right\} \quad (4)$$

Here, $M(G_n, W_u)$ is the multiplicative uncertainty set, G_n is nominal plant, W_u is multiplicative uncertainty weighting function, and G_a is the actual plant.

Considering the unmodeled dynamics and relative errors in high frequency, the input multiplicative weighing function is introduced as shown in Fig. 5. The maximum relative error for the weighting function is assumed to be 20% over 2.5 kHz.

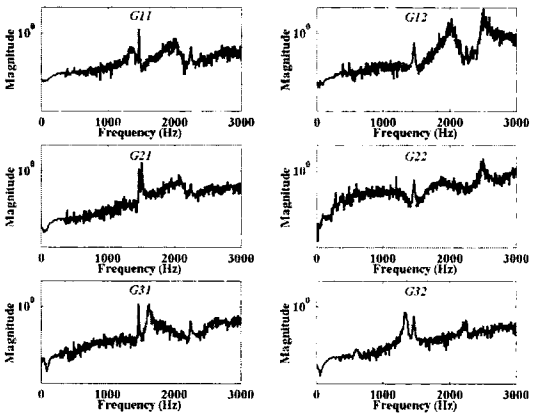

Fig. 4 Relative deviation of measured frequency responses

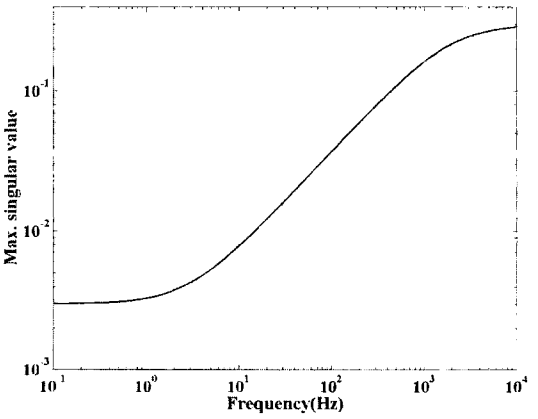

Fig. 5 Input multiplicative uncertainty weighting function for the unmodeled dynamics and relative errors in high frequency

3. Performance Weighting

A general closed-loop system is given in Fig. 6. Here, $G(s)$ is plant, $C(s)$ controller, w controller input disturbance, d plant input disturbance, n noise, y output, e controller input and u controller output. The closed-loop transfer function from input $[w, d, n]$ to output $[y, e, u]$ is given by Eq. (5).

$$\begin{bmatrix} y(s) \\ e(s) \\ u(s) \end{bmatrix} = \begin{bmatrix} T(s) & S(s)G(s) & T(s) \\ S(s) & S(s)G(s) & S(s) \\ C(s)S(s) & T(s) & C(s)S(s) \end{bmatrix} \begin{bmatrix} w(s) \\ d(s) \\ n(s) \end{bmatrix} \quad (5)$$

The minimization of the transfer function $S(j\omega)G(j\omega)$ is usually the main objective since it can be considered as stiffness of an AMB spindle from the unbalance force like disturbance d to the rotor displacement y. The control effort can be approximated by $C(j\omega)S(j\omega)$ since $S(j\omega) \approx 1$ over the cut-off frequency. Usually, the $C(j\omega)S(j\omega)$ is weighted to have a low pass characteristic in order to reject sensor noise, which is also extremely advantageous for controller order reduction and discrete time implementation.

Even though bounding of $S(j\omega)G(j\omega)$ and $C(j\omega)S(j\omega)$ already are sufficient to set up the μ synthesis (Fittro, 1998), an extended weighting scheme for the sensitivity function $S(j\omega)$ and the complementary sensitivity function $T(j\omega)$ additionally is very useful to obtain an reasonable controller. In addition, for the unstable plant with lightly damped modes like an AMB rotor system, this simple weighting scheme of bounding $S(j\omega)G(j\omega)$ and $C(j\omega)S(j\omega)$ gives us an unstable controller, which needs an additional simple controller like an PID controller for initial levitation. A sensitivity function $S(j\omega) > 1$ indicates that the

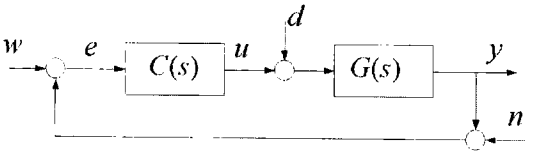

Fig. 6 Weighting schemes for closed-loop performance

controller is amplifying the disturbances that enter the system. Experience has shown that $S(j\omega)$ should be limited to approximately 3. For lightly damped flexible structures putting a strict bound on $C(j\omega)S(j\omega)$ will cause the resonances of plant to appear in $T(j\omega)$ with high peaks. The reason is that the all-pass property of H_∞ solution that bounds the shape of $C(j\omega)S(j\omega)$ exactly by pole-zero cancellation. Consequently, the resonances of plant appear by $T=GCS$ in $T(j\omega)$. This is undesired in all three meanings of $T(j\omega)$; reference action, the actuator response to disturbance and the transmission of sensor noise to the controlled variable. Hence, the bound on $C(j\omega)S(j\omega)$ is relaxed and a bound on $T(j\omega)$ with second-order low pass characteristics is introduced. (Schonhoff et al., 2000)

For SG-CS-S-T weighting scheme, the inputs w and d and output y, e and u should be chosen and augmented with the corresponding weighting functions. (Van Den Braembussche, 1998)

$$F_l(P, C)=\begin{bmatrix} W_yTW_w & W_ySGW_d \\ W_eSW_w & W_eSGW_d \\ W_uCSW_w & W_uTW_d \end{bmatrix} \tag{6}$$

Taking the criteria of selecting weighting functions into account, the weighting functions are tuned by trial and errors. The frequency responses of final weighting functions are shown in Fig. 7.

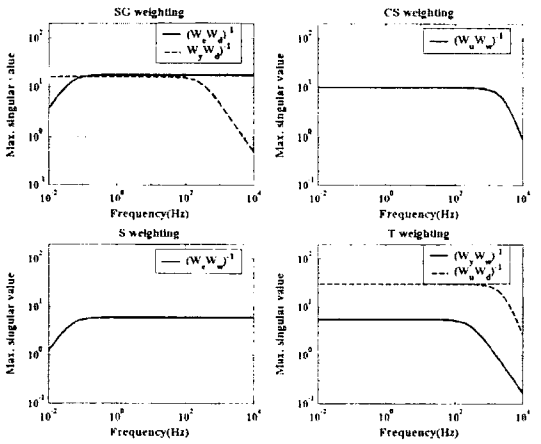

Fig. 7 Performance weighting functions

4. Controller Design

4.1 Augmentation

The nominal plant, the uncertainties and performance weighting functions are augmented before a robust control synthesis. To avoid being conservative, highly structured uncertainties are introduced. Table 3 shows the descriptions of the uncertainties.

The number of inputs and outputs related to uncertainties is 13 and the number of variables to describe uncertainties is also 13, which contains the 9 real uncertainties and 2×2 complex uncertainties. The number of inputs and outputs related to the performance weighting is 5 and 8, respectively. The fictitious uncertainty block for the robust performance is 8×5 full complex matrix. The robust control synthesis becomes two block problem according to the main loop theorem (Doyle et al., 1991). Block diagram of the augmented plant is shown in Fig. 8.

Table 3 The descriptions of uncertainties

Uncertainty		Description
Rotor	Real poles, δ_r	Two diagonal reqeated real uncertainties
	Complex poles, δ_f	Two diagonal real uncertainties
Sensor gain, δ_s		Two diagonal real uncertainties
Current gain, δ_k		Two diagonal real uncertainties
Input multiplicative uncertainty, δ_m		Full complex matrix uncertainties

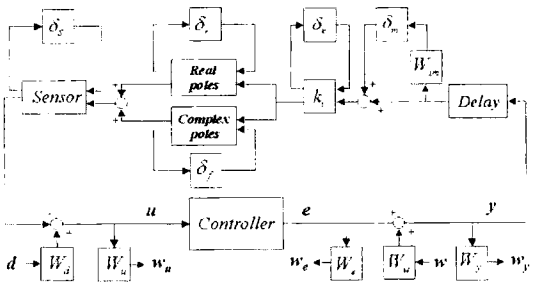

Fig. 8 Block diagram of the augmented plant

4.2 Mixed μ synthesis (Balas et al., 1995; Young 1996)

Since there is no direct mathematical solution of the μ synthesis problem, this problem is broken into two optimization problems. First, controller is fixed and the convex optimization of scaling matrix to minimize the cost function is performed. Second, scaling matrix is fixed and standard H_∞ optimization is solved. This iterative two step optimization procedure is known as D-K iteration. This procedure involves the D-K iteration between computing the μ upper bound, and solving an H_∞ (sub) optimal controller. This procedure does not guarantee to find the globally μ optimal controller, but has often been found to work well in practice.

In using the known structure of modeling error description of a system, conservatism associated with unstructured uncertainty can be considerably reduced through the structured singular value. Even if these procedures offer great proceeds towards reducing unnecessary conservatism, a major limitation is obvious since the μ analysis and synthesis were developed based on the assumption that every individual uncertainty block is complex. However, in specific applications it may be more reasonable to use some of the uncertainties with real perturbations. While it is possible to simply treat these perturbations as complex and proceed with the complex μ synthesis, result can be expected to be conservative. However, the complex μ synthesis procedure has been successfully applied to a large number of engineering problems. By using some new analysis tools recently developed for the mixed μ upper bound, the mixed uncertainty problem can be tractable without expectation of conservatism due to the complex μ synthesis. D, G-K iteration which finds a controller that stabilizes the nominal system and attempts to minimize the peak values (across frequency) of mixed μ. Contrary to complex μ synthesis, another scaling matrix G is introduced for real uncertainties. Mixed μ synthesis can be broken down into two sub problems. Firstly, for a fixed controller, two scaling matrices can be obtained point wise in frequency through convex optimization. Secondly, fixing scaling matrices, the controller can be solved through the standard H_∞ optimization.

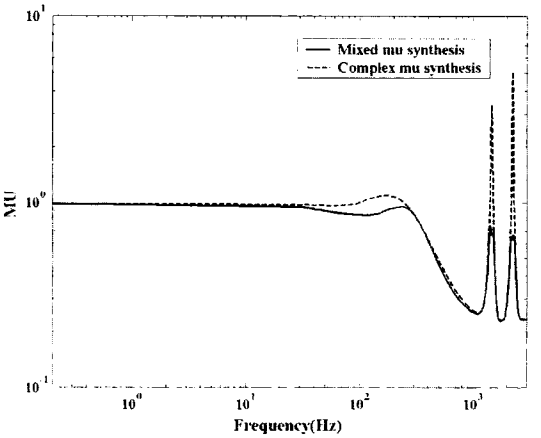

Fig. 9 Mixed and complex μ synthesis

Figure 9 shows the achieved μ values of the complex and mixed μ synthesis. The mixed μ synthesis enables us to avoid being too conservative. Especially since the small perturbation causes a large change of frequency responses for the lightly damped flexible system, the mixed μ synthesis and highly structured uncertainty description should be used.

4.3 Controller order reduction (Wortelboer, 1994)

The demand of an accurate plant model in order to achieve robust performance comes along with high order models. In addition, there are the restrictions of model reduction in advance of the controller design. However, as well as accurate modeling is demanded for reliable application, a low order of the controller is prerequisite for economic realization. In addition, the μ synthesis results in a huge and complex controller since the order of the controller is that of augmented plant plus the D-scales fitted during D-K iteration. Therefore, controller reduction is an inevitable step and the balanced truncation method has become common practice. However, in order to preserve the robust performance of the original controller, it is natural to adopt the below minimization scheme.

$$Min\ \sup(\mu_\Delta(F_l(G, C) - F_l(G, C_r))) \quad (12)$$

By replacing μ with its upper bound and using the D-scaling as in the D-K iteration, the minimization problem can be formulated in terms of rational transfer functions.

$$Min \| D_l F_l(G, C) D_r^{-1} - D_l F_l(G, C_r) D_r^{-1} \|_\infty \quad (13)$$

This can directly be tackled by a frequency weighted balanced reduction in closed loop configuration. Using this scheme a significant reduction of the controller can be achieved without major loss of the performance.

The designed original controller of 28th order can be reduced to the half order without any significant performance degrades. The frequency responses of the original and reduced controller are shown in Fig. 10. There is not any significant difference between original and reduced controller up to the controller bandwidth, 3 kHz. The μ analysis results of the original and reduced controller are shown in Fig. 11. The reduced controller satisfies the robust stability and performance criteria.

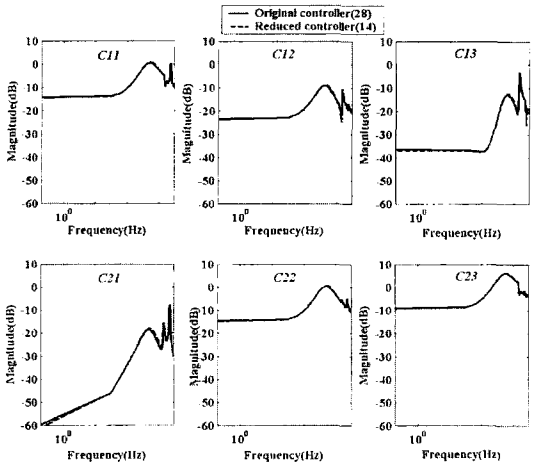

Fig. 10 The original and reduced controllers

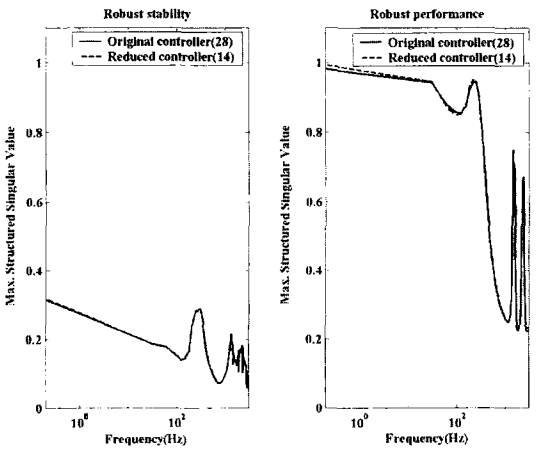

Fig. 11 Comparisons of the original and reduced controllers (a) Robust stability (b) Robust performance

4.4 Implementation

To implement the designed robust controller, a DSP board based on TMS320C44 and two 4 channel AD/DA (Innovative Integration co., 1998) are used. The assembly language (Texas Instruments Co., 1995) is used in the time critical control routine to implement the complex controller within the sampling time. Other jobs including DFT calculation of the captured data for identification, gain tuning, display and writing of the experimental results are written in C language. These routines are not first priority and run in the intermediate time between the time critical control routines.

4.5 Controller validation

To validate performances of the real plant, the closed loop responses related to the performance weightings are measured experimentally. The measured closed loop responses and the performance

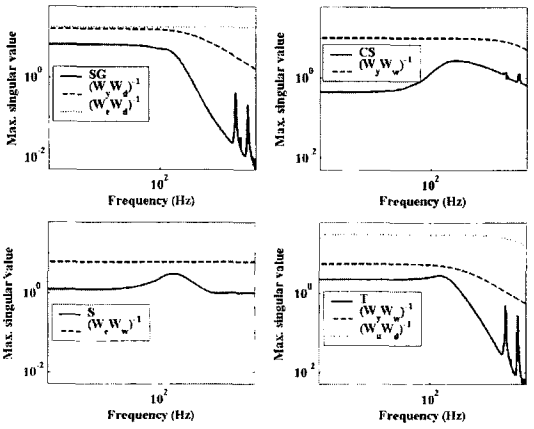

Fig. 12 Weighting functions and measured closed-loop frequency responses

weighting functions are shown in Fig. 12. The closed loop responses of the actual plant satisfy the performance specifications of the weighting functions.

5. Experiments

5.1 Benchmark PID controller

To compare the performance of the designed μ controller, a benchmark PID controller is designed. Since the rotor motion is measured in three points, a linear interpolation of front and middle sensors is used as the input of the PID controller for the front bearing. The frequency response of the PID controller is shown in Fig. 13. The AMB spindle with the PID controller can be operated up to 850 Hz because of the conical mode vibration.

5.2 Comparison with the benchmark PID controller

5.2.1 Unbalance responses

Figure 14 shows unbalance responses of the PID and μ controllers with the increase of rotational speed up to 960 Hz, which is the maximum speed of the used inverter. Typical two rigid modes appear in the PID controller ; translation mode near at 100 Hz and conical mode near at 860 Hz. Although there are also rigid modes with the μ controller, the maximum vibration amplitudes in the rigid modes are a little bit decreased.

5.2.2 Control efforts

The control efforts are shown in Fig. 15. The μ controller gives more control efforts than PID controller, which means higher gain and stiffness. The asymmetry in control efforts of two bearings is bigger in the PID control than the μ controller, which means efficient use of bearing forces in the μ controller. This result can be explained by the off-diagonal components of the μ controller.

5.2.3 Radial error motions

The radial error motions of the AMB spindle with various rotational speeds are shown in Fig. 16. Translational resonance due to the rigid mode

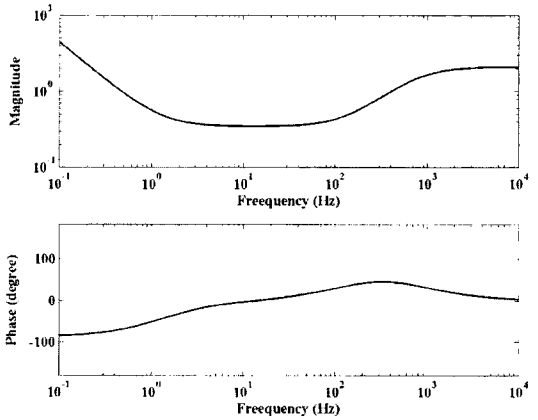

Fig. 13 Frequency response of the benchmark PID controller

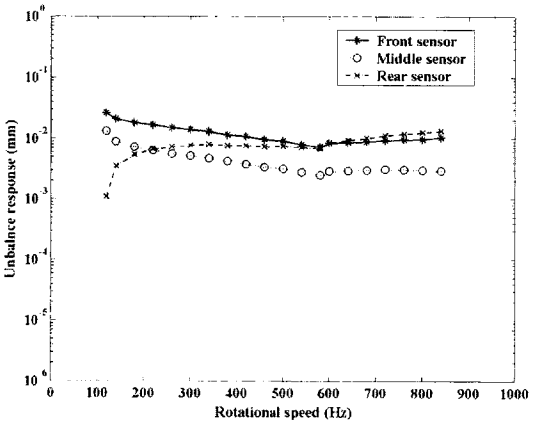

(a) The PID control

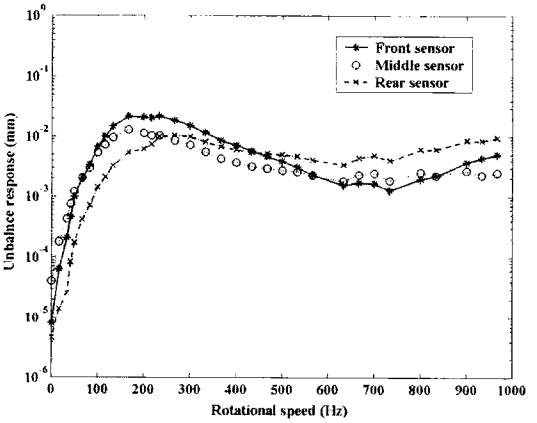

(b) The μ control

Fig. 14 Unbalance responses with the PID and μ controller

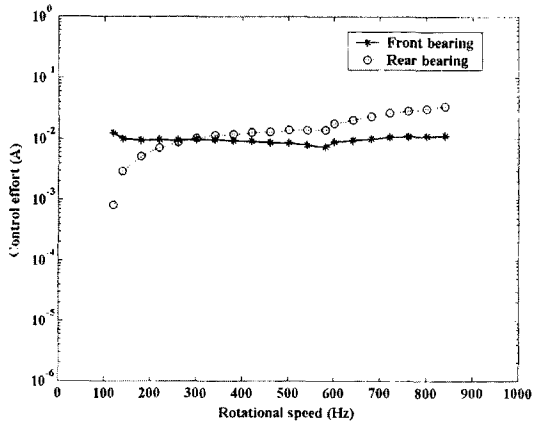

(a) The PID control

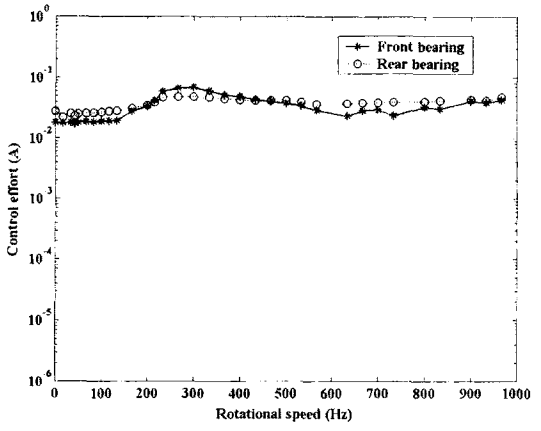

(b) The μ control

Fig. 15 Control efforts with PID and μ controller

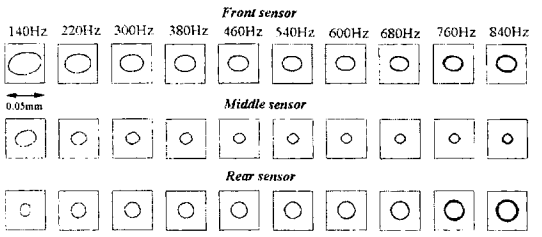

(a) The PID control

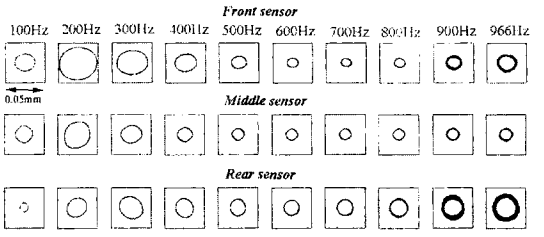

(b) The μ control

Fig. 16 Radial error motions of rotor with the PID and μ controller

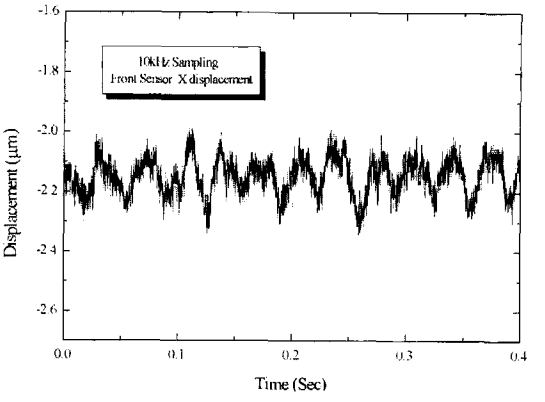

Fig. 17 Stationary suspension noise of the CCS

is near 100 Hz in PID controller and 200 Hz in μ controller. The orbits possess almost circular shapes, which is due to the spatial average effect of the CCS. The geometric errors of rotor are reduced considerably with CCS and only real rotor motion is measured. The unbalance response of the μ controller is a little bit smaller than that of the PID controller at the same rotating speeds : especially in the front sensor. This comes from higher stiffness of the μ controller, more flexible structure of using off-diagonal control and more weighting due to two fromt sensor inputs.

5.2.4 Sensor performance with the suspension control

The controller is implemented, and the stationary suspension noise is measured. and shown in Fig. 17. The accuracy of the static suspension is less than 0.3 μm.

6. Conclusion

This paper discusses an entire procedure for a robust controller design and its implementation of an AMB spindle. Various uncertainties for the AMB spindle were tightly evaluated based on the experimental results of part I, and an appropriate performance weighting scheme for the AMB spindle was developed. A designed robust control

through the mixed μ synthesis was reduced considering closed loop performances and was implemented into the AMB spindle. Experimental justification of the designed robust controller is performed through measuring closed-loop frequency responses. The AMB spindle was operated up to 57,600 rpm and performance of the designed controller was compared with a benchmark PID controller through experiments. Experiments show that the robust controller offers higher stiffness and more efficient control of rigid modes than the benchmark PID controller.

References

Ahn, H. J., Jeon, S. and Han, D. C., 2000, "Error Analysis of the Cylindrical Capacitive Sensor for Active Magnetic Bearing Spindles," *J. of Dynamics systems, measurement, and control*, trans. of ASME, March, Vol. 122, pp. 102~107.

Balas, G. J., Doyle, J. C., Glover, K., Packard, A. K. and Smith, R., μ-Analysis and Synthesis toolbox, the MathWorks, Natick, MA, 1995.

Balas, G. J. and Young, P. M., 1995, "Control Design for Variations in Structural Natural Frequencies," *Journal of Guidance, Control and Dynamics*, Vol. 18, No. 2, pp. 325~332.

Carrere, F., Font, S. and Duc, G., 1994, "H_∞ Control Design of Flexible Rotor Magnetic Bearing System," *Proceedings of the 4th ISMB*, Zurich, Switzerland, pp. 65~71.

Cui, W. M. and Nonami, K., 1992, "H_∞ Control of Flexible Rotor-Magnetic Bearing Systems," *Proceedings of the 3rd ISMB*, Alexandria, Virginia, USA, pp. 504~514

Doyle, J., Packard, A. and Zhou, K., 1991, "Review of LFTs, LMIs, and μ," *Proceedings of the 30th Conference on Decision and Control*, Brington, England.

Fittro, R. L., 1998, "A High Speed Machining Spindle with Active Magnetic Bearings : Control Theory, Design, and Application," Ph. D. dissertation, University of Virginia, USA.

Innovative Integration Co., 1998, M44 DSP Hardware manual, USA.

Jeon, S., Ahn, H. J., Chang, I. B. and Han, D. C., 2001, "A New Design of Cylindrical Capacitive Sensor for On-line Precision Control of AMB Spindle," *IEEE Transactions on Instrumentation and measurement*, Vol. 50, No. 3, pp. 757~763.

Jeon, S., Ahn, H. J. and Han, D. C., 2003, "Control of Flexible Rotor with Active Magnetic Bearing System," KSME International Journal, 16(12), pp. 1583~1593.

Kim, S. J. and Lee, C. W., 1998, "On-line Identification of Position and Current Stiffnesses in Active Magnetic Bearing System Equipped with Built-in Force Transducers by LMS Algorithm," *Transactions of KSME A.*, 22(12), pp. 2261~2268.

Losch, F., Gahler, C. and Herzog, R., 1998, "μ-Synthesis Controller Design For a 3MW Pump Running In AMBs," *Proceedings of the 6th ISMB*, MIT, Massachusetts, USA, pp. 415~428.

Namerikawa, T., Fugita, M. and Matsumura, F., 1998, "Uncertainty Structure and μ-Design of a Magnetic Suspension System," *Proceedingsof the 6th ISMB*, MIT, Boston, MA, USA, pp. 439~447.

Nonami, K., Ueyama, H. and Yutaka, S., 1994, "H_∞ Control of Milling AMB Spindle," *Proceedings of the 4th ISMB*, Zurich, Switzerland, pp. 531~536.

Nonami, K., Takayuki, I., 1994, "μ Synthesis of Flexible Rotor Magnetic Bearing Systems," *Proceedings of the 4th ISMB*, Zurich, Switzerland, pp. 73~78.

Stephens, L. S., 1995, "Design and Control of Active Magnetic Bearings for a High Speed Machining Spindle," Ph. D. dissertation, University of Virginia, USA.

Schonhoff, U., Luo, J., Li, G., Hilton, E., Nordmann, R. and Allaire, P. E., 2000, "Implementation Results of μ-Synthesis Control for an Energy Storage Flywheel Test Rig," *Proceedings of the 7th ISMB*, Zurich, Switzerland, pp. 317~322.

Texas Instruments Co., 1995, TMS 320C4x User's Guide, USA.

Van Den Braembussche, P., 1998, "Robust Motion Control of High Performance Machine Tools with Linear Motors," Ph. D. dissertation, Katholieke Universiteit Leuven, Belgium.

Wortelboer, P. M. R., 1994, "Frequency-weighted Balanced Reduction of Closed-loop Mechanical Servo- systems : Theory and Tools," Ph. D. dissertation, Delft University of Technology, Nederland.

Young, P. M., 1996, "Controller Design with Real Parametric Uncertainty," *International Journal of Control*, Vol. 65, No. 3, pp. 469~509.